Lattice Distortions Induced by As^{3+}, Sb^{3+}, and Bi^{3+} Substitutional Impurities in KCl: An Embedded Cluster Study

Andrés Aguado*

Physical and Theoretical Chemistry Laboratory, University of Oxford, South Parks Road, Oxford OX1 3QZ, U.K.

Received: January 11, 2002; In Final Form: April 12, 2002

An embedded cluster analysis of the lattice distortions induced by As^{3+}, Sb^{3+}, and Bi^{3+} substitutional impurities in crystalline KCl is presented. Active clusters containing more than 100 atoms that are embedded in a quantum representation of the crystalline environment are used. Charge compensation is achieved by introducing two cation vacancies in the host lattice, both in nearest-neighbor (NN) and next-nearest-neighbor (NNN) configurations. Distortion trends as a function of the impurity cation size are identified and discussed, as well as the relative stability of the NN and NNN configurations.

I. Introduction

Ionic crystals doped with substitutional impurities have optical absorption and emission properties that are different from those of the pure crystals, a finding that has very important implications in the field of luminescent materials.[1] In particular, the electronic spectra of alkali halide crystals doped with Tl^+-like substitutional impurities have been experimentally characterized in the past.[2−4] It is known that these spectra are strongly coupled with the crystal field and thus are quite sensitive to the lattice distortions around the impurity. Much less is known, however, about the detailed local distortion induced by the introduction of the dopant. Employment of an extended X-ray absorption fine structure (EXAFS) technique would allow, in principle, the experimental measurement of these distortions, but in practice, this is difficult in many cases, for example, when the impurity concentration is low[5−7] or when two or more impurity charge states coexist.[8] This is the main reason that reliable ab initio calculations of the local structure around defects are both timely and desirable.

Most of the experimental measurements referred to above have been involved with isovalent (Ga^+, In^+, Tl^+, Cu^-, Ag^-, Au^-) and doubly charged aliovalent (Ge^{2+}, Sn^{2+}, Pb^{2+}) Tl^+-like impurities. The structural distortions induced by these impurities in a variety of alkali halide crystals have also been analyzed from a theoretical point of view. In the case of isovalent impurities in their ground ns^2 electronic configuration, it is mainly the size mismatch between impurity and host ions that determines the lattice distortion, which is a radial breathing displacement of several coordination shells of ions about the impurity.[9−11] With increasing concentration of the dopant, aggregation of impurity centers will eventually appear. The spectroscopic properties of Tl^+-dimer centers, for example, have been experimentally determined.[12] The lattice distortions induced by these dimer centers have also been addressed by electronic structure methods.[13] When the impurity is doubly charged, the problem of charge compensation emerges. Usually, charge compensation is achieved by the creation of a cationic vacancy in the host lattice.[3,4,14−27] That vacancy can be in nearest-neighbor (NN) or next-nearest-neighbor (NNN) positions,[26] and it induces a static crystal field of symmetry lower than cubic. The unbalanced electric field also induces an off-center displacement of the impurity ion, which is detectable in ionic thermocurrent experiments.[26] Theoretical consideration of the lattice distortions induced by doubly charged aliovalent impurities in alkali halides and of the off-center equilibrium position adopted by these cations has also been undertaken by us in previous work.[28] It was found that the electrostatic effects associated with the aliovalent character of the impurity are more important than the size mismatch effect in determining the distortions.

Many fewer studies have been devoted to the optical properties of alkali halide crystals doped with triply charged aliovalent (As^{3+}, Sb^{3+}, Bi^{3+}) impurities. The optical absorption spectra of NaCl/Sb^{3+} have been examined by Radhakrishna and Karguppikar,[29] whereas Choi et al.[30] presented results for KCl/Sb^{3+} and KI/Sb^{3+}. Some papers dealing with the absorption of Bi^{3+} cations have also been published.[31−33] More recently, Tsuboi et al.[34] have presented a more detailed study of the absorption bands in KCl/Sb^{3+}, and Kang et al.[35] have considered both absorption and emission spectra of KCl/Bi^{3+}. Substitution of triply charged ions into an alkali halide lattice is accompanied by the creation of two cation vacancies, which can be allocated in the first (NN) or second (NNN) cation coordination shells about the impurity. Tsuboi et al.[34] observed that the effect of these two vacancies on the obtained spectra was smaller than that in the case of doubly charged impurities. Also, Kang et al.[35] stressed that it is necessary to know which of the two different configurations of the vacancies is energetically preferred to make a precise assignment of the experimental absorption−emission bands. To the best of our knowledge, however, no electronic structure calculations on the lattice distortions have been published for this kind of system.

In this paper, we have employed the ab initio perturbed ion (aiPI) model[36−41] to study the lattice distortions induced by As^{3+}, Sb^{3+}, and Bi^{3+} in KCl, both in NN and NNN configurations. Our main goals are to try to rationalize the observed distortion patterns and to study the relative stability of these two defect geometries. In this way, we provide the first electronic structure calculations on these systems. The remainder of this paper is organized as follows. In section II, we give a brief account of

* E-mail: aguado@joule.pcl.ox.ac.uk.

10.1021/jp020076c CCC: $22.00
Published on Web 06/21/2002

TABLE 1: Lattice Distortions (in Å) of Several Coordination Shells around As^{3+}, Sb^{3+}, and Bi^{3+} in KCl, with Cation Vacancies at the (0 0 1) and (0 0 −1) Lattice Sites[a]

coordination shell	ionic site	deg	pure-crystal values	distortion	As	Sb	Bi
first	$(U_1\ 0\ 0)$	4	$U_1 = 1/2$	ΔU_1	−0.687	−0.600	−0.519
	$(0\ 0\ U_2)$	2	$U_2 = 1/2$	ΔU_2	−0.734	−0.649	−0.569
	$(0\ 0\ U_3)$	2	$U_4 = 3/2$	ΔU_3	0.248	0.243	0.240
	$(U_4\ 0\ U_5)$	8	$U_4 = 1/2$	ΔU_4	0.291	0.299	0.305
			$U_5 = 1$	ΔU_5	0.003	0.013	0.022
second	$(U_1\ U_1\ 0)$	4	$U_1 = 1/2$	ΔU_1	0.150	1.171	0.181
	$(U_2\ 0\ U_3)$	8	$U_2 = 1/2$	ΔU_2	0.068	0.093	0.109
			$U_3 = 1/2$	ΔU_3	0.247	0.268	0.284
	$(U_4\ U_4\ U_5)$	8	$U_4 = 1/2$	ΔU_4	0.006	0.005	0.009
			$U_5 = 1$	ΔU_{5q}	0.114	0.118	0.125
	$(U_6\ 0\ U_7)$	8	$U_6 = 1/2$	ΔU_6	−0.028	−0.027	−0.019
			$U_7 = 3/2$	ΔU_7	0.073	0.078	0.080
third	$(U_1\ U_1\ U_2)$	8	$U_1 = 1/2$	ΔU_1	−0.122	−0.133	−0.139
			$U_2 = 1/2$	ΔU_2	−0.163	−0.175	−0.179
	$(U_3\ U_3\ U_4)$	8	$U_3 = 1/2$	ΔU_3	−0.048	−0.049	−0.046
	$(U_3\ U_3\ U_4)$	8	$U_3 = 1/2$	ΔU_3	−0.048	−0.049	−0.046
			$U_4 = 3/2$	ΔU_4	−0.052	−0.053	−0.054
fourth	$(U_1\ 0\ 0)$	4	$U_1 = 1$	ΔU_1	0.275	0.275	0.266
	$(0\ 0\ U_2)$	2	$U_2 = 2$	ΔU_2	0.216	0.217	0.210
	$(U_3\ 0\ U_4)$	8	$U_3 = 1$	ΔU_3	0.222	0.230	0.229
			$U_4 = 1$	ΔU_4	0.136	0.140	0.141

[a] The optimization parameters, U_i, together with their pure crystal values in crystallographic units, are shown explicitly, as well as the number of symmetry-equivalent ions in each coordination shell.

the theoretical model employed. In section III, we present and discuss the results of the calculations, and in section IV, we summarize the main conclusions.

II. Theory: Cluster Model

The aiPI model is a particular application of the theory of electronic separability of Huzinaga and co-workers[42,43] to ionic solids in which the basic building blocks are reduced to single ions. The PI model was first developed for perfect crystals.[36] Its application to the study of impurity centers in ionic crystals has been described in refs 44−46. The theoretical details of the model have been explained at length in one of our previous publications,[13] so we refer the reader to this work for a fuller account of the method.

The active clusters employed in this work to represent the local distortions around NN and NNN defects have been constructed following well-defined physical rules: (a) they are embedded in accurate quantum environments including Coulombic, exchange, and orthogonality effects;[11] (b) the active space is split into two subsets that we refer to as $\mathbf{C}_1$ and $\mathbf{C}_2$, following the notation in refs 44 and 45. Both the positions and wave functions of the ions in the inner $\mathbf{C}_1$ subset are allowed to relax. The positions of the ions in the outer $\mathbf{C}_2$ subset are fixed during the optimization process, but their wave functions are self-consistently optimized. Thus, the $\mathbf{C}_2$ subset provides a smooth interface connecting the $\mathbf{C}_1$ region, where distortions are important, to the frozen crystalline environment. In practice, $\mathbf{C}_2$ contains all those ions that are first neighbors of the ions in $\mathbf{C}_1$ and are not already contained in $\mathbf{C}_1$. This completely defines the $\mathbf{C}_2$ subset for each of the cluster models. We still have to specify the $\mathbf{C}_1$ subset used to represent the NN and NNN defects. To do this, let us define the *n*th coordination shell of the complex formed by the impurity and the two vacancies as that set of ions containing all of the *n*th nearest neighbors of *both* the impurity *and* the vacancies. Then, we have chosen to include in the $\mathbf{C}_1$ subset the first four coordination shells of the defect complex. The total number of ions thus included in the active clusters is 177 and 151 for the NNN and NN defects, respectively. The energy minimization procedure employed to optimize the positions of the ions in the different coordination shells is also the same as that employed in previous publications.[13] The basis sets employed to represent the ions have been taken from the compilations of Clementi and Roetti[47] and McLean and McLean.[48]

Taking into account small self-embedding corrections,[9−11] the distortions have been calculated using the equation

$$\Delta U_i = U_i(\mathrm{KCl{:}\ Imp^{3+}}) - U_i(\mathrm{KCl{:}\ K^{+}}) \qquad (1)$$

where U_i are the structural parameters employed to characterize the geometry of the active cluster (see next section). In this way, both pure and doped crystals are treated equally in eq 1. Our decision to use the aiPI model to solve the electronic structure of the active cluster is motivated by our interest in structural properties. The atomic character of the aiPI model[44−46,13] results in a linear scaling of the computational effort with the number of symmetry-equivalent atoms. This scaling is very important when the distortions are long-ranged and a large number of ions have to be explicitly described. In our case, active clusters containing more than 100 atoms are considered. Another important factor is the dimensionality of the potential energy surface. The structural characterization of some of the defects described below involves energy optimizations in parametric hyperspaces with more than 20 dimensions. Clearly, the employment of more sophisticated molecular orbital calculations, like those based on the linear combination of atomic orbitals (LCAO) approximation, would be prohibitive.

III. Results and Discussion

A. Cation Vacancy in the NNN Position. We show in Table 1 the equilibrium values of the 20 parameters describing the lattice distortions induced by the NNN defects. A 3-D pictorial view of the ions in the $\mathbf{C}_1$ subset is also given in Figure 1 for the case of KCl/Sb^{3+}. The first coordination shell of the impurity experiences a large contraction in all cases, which is larger the smaller the size of the impurity. This trend can be explained by the competition of two physical effects: (a) on one hand, the increased Madelung potential of the impurity, as compared

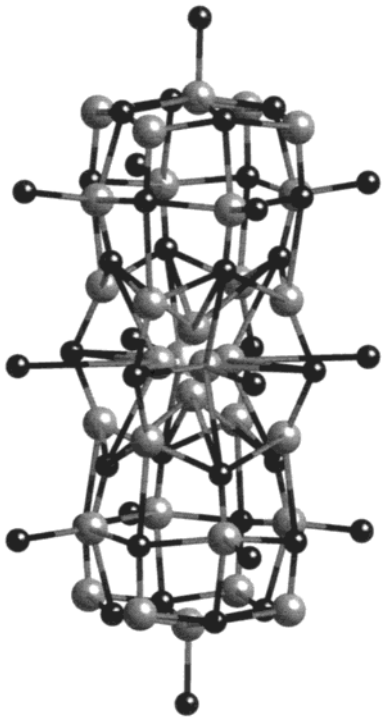

Figure 1. Graphical 3-D visualization of the lattice distortions induced by Sb^{3+} in KCl, with the cation vacancies located along the (0 0 1) crystallographic direction. All ions inside the $\mathbf{C}_1$ subset are shown (see text). Distortions have been exaggerated by a factor of 3 to make them more visible. Small black spheres represent K^+ cations, big gray spheres represent Cl^- anions, and the central, light gray sphere represents the Sb^{3+} cation.

to that of the host cation, tends to contract the first coordination shell (formed by anions) in the three systems; (b) on the other hand, there is a size mismatch between the impurity and the host cation. This mismatch is largest in KCl/Bi^{3+} and smallest in KCl/As^{3+}, which explains the main observed trend. We also observed that, for every impurity cation, the contraction is the largest for the two anions in (0 0 $^1/_2$) crystallographic sites because of the negative effective charge of the two cation vacancies. The two anions in (0 0 $^3/_2$) crystallographic sites also experience an expansion due to the unbalanced Madelung field. This expansion is almost completely independent of the specific substitutional impurity, that is, it is a purely electrostatic effect. Finally, the eight anions at ($^1/_2$ 0 1) and equivalent positions undergo an in-plane expansion due to the effect of the vacancy and also a small off-plane displacement. The distortions depend on the impurity because of coupling with second-shell distortions, as we will explain in the following paragraph.

The 12 cations in the second coordination shell about the impurity experience an expansion that results from the conjoint action of two physical effects: (a) The increased Madelung repulsion induces an important expansion of the second shell. Indeed, this expansion is found to be larger than that in similar isovalent cases.[9−11] Thus, an explicit consideration of second-shell distortions seems mandatory in the case of aliovalent impurities. (b) The increased overlap repulsion due to the size mismatch effect induces further expansion. The decrease in the size mismatch along the series $Bi^{3+}-Sb^{3+}-As^{3+}$ explains the main observed trend. We also noticed that the expansion of the eight cations in ($^1/_2$ 0 $^1/_2$) crystallographic sites proceeds mainly along the *z* axes because the negative effective charge of the vacancies attracts these cations. The size mismatch effect in the expansion of these eight cations induces a coupling with the distortion of the first-shell anions in ($^1/_2$ 0 1) positions, explaining the dependence of the first-shell distortions on the chemical identity of the dopant. The eight cations at ($^1/_2$ $^1/_2$ 1) sites, which are in the second coordination shell of the vacancies, show almost no in-plane distortion. Their natural tendency would be to approach the negative effective charge of the vacancy, but this approach is impeded by the large expansion of the first-shell anions at ($^1/_2$ 0 1) positions (yet another case of coupling between shells). A similar effect explains the expansion of the cations along the *z* axes. Finally, the eight cations at ($^1/_2$ 0 $^3/_2$) and equivalent sites show an in-plane tendency to approach the cation vacancies, which is overweighed by an expansion along the *z* axes that is dictated again by complicated couplings to the other shells so that an intuitive explanation of the distortions becomes difficult to obtain.

The eight anions at ($^1/_2$ $^1/_2$ $^1/_2$) positions are in the third coordination shell of both the impurity and one of the vacancies. The contraction of these ions can be rationalized in terms of the increased Madelung field of the impurity and the negative effective charge of the vacancy. Thus, the contraction is larger along the *z* axes compared to the contraction within the *xy* plane. These anions do not overlap the electronic cloud of the impurity, so the small differences observed among the three materials should be related to couplings with first- and second-shell distortions. In particular, the contraction increases with the size of the impurity. This behavior has also been observed for isovalent impurities,[11] for which it was concluded that the larger expansion of the second shell with increasing impurity size makes enough room for further contraction of the third-shell anions.

The four cations at (1 0 0) sites experience an appreciable expansion as a result of the increased Madelung field, which is not very sensitive to the specific substitutional impurity. The rest of the cations in the fourth shell expand as a consequence of the expansion of the anions in the first coordination shell about the impurity.

B. Cation Vacancy in NN Position. When the vacancies are in NN positions, the number of symmetry equivalences is further reduced, and a total of 28 parameters are needed to optimize the local geometry. The equilibrium values of these parameters are shown in Table 2, whereas a graphical representation of the distortions in 3-D is given in Figure 2. The very general features of the distortions are quite the same as in the case of the NNN defect; for example, the first coordination shell of anions about the impurity contracts, and this contraction is larger the smaller the size of the impurity. The differences arise as a consequence of the different symmetries of the defects, so we will focus here only on a description of these differences. The two anions at (0 0 $^1/_2$) sites experience a contraction that is almost indistinguishable from that observed in the NNN case for the four anions that are less affected by the vacancies (compare Tables 1 and 2). The four anions at ($^1/_2$ 0 0) and equivalent positions undergo both a contraction and an off-axis displacement induced by the negative effective charge of the vacancies. The behavior of the four anions at ($^1/_2$ $^1/_2$ $^1/_2$) and equivalent sites, which are in the third coordination shell about the impurity but in the first coordination shell about one vacancy, is also interesting. They experience an expansion along the *z* axis (driven by the negative effective charge of the vacancy) and a contraction in the *xy* plane that serves to approach the increased Madelung field of the impurity.

Let us briefly discuss the distortion in the other shells. Regarding the second shell, the two cations at ($^1/_2$ $-^1/_2$ 0) positions are the only ones that are not significantly affected by the vacancies and undergo a simple expansion along the (1

TABLE 2: Lattice Distortions (in Å) of Several Coordination Shells around As^{3+}, Sb^{3+}, and Bi^{3+} in KCl, with Cation Vacancies at the ($^1/_2$ $^1/_2$ 0) and ($-^1/_2$ $-^1/_2$ 0) Lattice Sites

coordination shell	ionic site	deg	pure-crystal values	distortion	As	Sb	Bi
first	(U_1 U_2 0)	4	$U_1 = {}^1/_2$	ΔU_1	−0.707	−0.622	−0.528
			$U_2 = 0$	ΔU_2	−0.115	−0.140	−0.199
	(0 0 U_3)	2	$U_3 = {}^1/_2$	ΔU_3	−0.685	−0.601	−0.517
	(U_4 U_5 0)	4	$U_4 = 1$	ΔU_4	0.248	0.253	0.274
			$U_5 = {}^1/_2$	ΔU_5	−0.045	−0.049	−0.060
	(U_6 U_6 U_7)	4	$U_6 = {}^1/_2$	ΔU_6	−0.053	−0.068	−0.122
			$U_7 = {}^1/_2$	ΔU_7	0.289	0.276	0.238
second	(U_1 $-U_1$ 0)	2	$U_1 = {}^1/_2$	ΔU_1	0.134	0.162	0.184
	(U_2 U_3 0)	4	$U_2 = 1$	ΔU_2	0.177	0.171	0.174
			$U_3 = 0$	ΔU_3	0.071	0.069	0.053
	(U_4 U_5 U_4)	8	$U_4 = {}^1/_2$	ΔU_4	0.095	0.120	0.157
			$U_5 = 0$	ΔU_5	0.111	0.102	0.070
	(U_6 U_6 0)	2	$U_6 = 1$	ΔU_6	0.008	0.013	0.023
	(U_7 U_8 U_9)	8	$U_7 = 1$	ΔU_7	0.048	0.053	0.067
			$U_8 = {}^1/_2$	ΔU_8	0.039	0.040	0.042
			$U_9 = {}^1/_2$	ΔU_9	−0.016	−0.018	−0.014
third	(U_1 $-U_1$ U_2)	4	$U_1 = {}^1/_2$	ΔU_1	−0.171	−0.168	−0.158
			$U_2 = {}^1/_2$	ΔU_2	−0.111	−0.116	−0.112
	(U_3 U_3 U_4)	4	$U_3 = 1$	ΔU_3	−0.063	−0.066	−0.071
			$U_4 = {}^1/_2$	ΔU_4	−0.042	−0.041	−0.040
	(U_5 U_6 U_7)	8	$U_5 = 1$	ΔU_5	−0.090	−0.081	−0.058
			$U_6 = 0$	ΔU_6	−0.002	−0.003	−0.004
			$U_7 = {}^1/_2$	ΔU_7	−0.092	−0.090	−0.084
fourth	(0 0 U_1)	2	$U_1 = 1$	ΔU_1	0.248	0.243	0.236
	(U_2 U_3 0)	4	$U_2 = {}^3/_2$	ΔU_2	0.222	0.223	0.227
			$U_3 = {}^1/_2$	ΔU_3	0.048	0.048	0.042
	(U_4 U_4 U_5)	4	$U_4 = {}^1/_2$	ΔU_4	0.093	0.092	0.088
			$U_5 = 1$	ΔU_5	0.217	0.216	0.207

[a] The optimization parameters, U_i, together with their pure crystal values in crystallographic units, are shown explicitly, as well as the number of symmetry-equivalent ions in each coordination shell.

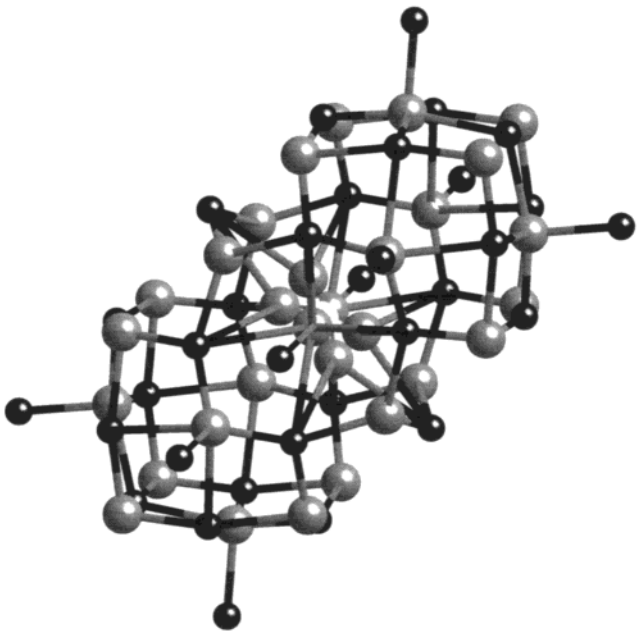

Figure 2. Graphical 3-D visualization of the lattice distortions induced by Sb^{3+} in KCl, with the cation vacancies located along the (1 1 0) crystallographic direction. The description is the same as in Figure 1.

−1 0) crystallographic direction, which increases with the size of the impurity. The distortion of the rest of the cations in this shell can be simply understood as the coupled effects of the electrostatic fields of the impurity and the vacancies. For example, a cation at ($^1/_2$ 0 $^1/_2$) undergoes an expansion that is larger along the *y* axis because in this way it approaches the negative effective charge of one vacancy. A cation at (1 0 0) expands along the *x* axis but also approaches one of the vacancies along the *y* axis. Those cations at (1 1 0) positions do not displace appreciably because the attraction due to the vacancies is largely canceled by the impurity repulsion in this particular geometry. Third- and fourth-shell distortions are more difficult to analyze because we also have to consider the coupling to inner-shell distortions. For example, considering now the third shell, the four anions at ($^1/_2$ $-^1/_2$ $^1/_2$) and equivalent sites experience a contraction to approach the impurity. This contraction is smaller along the *z* axis because of the expansion of the two second-shell cations at ($^1/_2$ $-^1/_2$ 0), which reduces the screening between the two anions with different *z* coordinates. Similar arguments (more or less complicated) serve to explain the rest of the distortions.

C. Discussion of the Relative Stabilities of NN and NNN Defect Configurations. A highly relevant issue is the relative stability of the different defect configurations, that is, the energetically preferred allocation of the cationic vacancies with respect to the impurity ion. At low pressure and temperature conditions, the formation of the impurity centers should be discussed in terms of the internal energy difference for the exchange reaction

$$\mathrm{KCl/K_s^+} + \mathrm{Imp_g^{3+}} \rightleftharpoons \mathrm{KCl/Imp_s^{3+}} + 3\mathrm{K_g^+} \qquad (2)$$

where the s and g subscripts refer to solid and gas phases, respectively. We note here that the complex formed by the impurity and the two vacancies creates a quadrupolar field that polarizes the rest of the ionic lattice, and this polarization may have an effect on the formation energies. A solution to this problem is to couple the quantum mechanical representation of the active cluster to a phenomenological shell-model description of lattice polarization.[49] In this paper, as the size of the active clusters is already quite large, only intracluster polarization has been included. As a model for polarization, we have chosen

the model introduced by Madden and co-workers,[50−53] as described in detail in previous work.[13,54] We have calculated the formation-energy difference between NN and NNN defect configurations and have found that the NN configuration is more stable in all three cases by an amount (0.51 eV) that is quite independent of the specific impurity.

We already found in the case of doubly charged aliovalent impurities[28] that purely electrostatic effects are more important in determining distortions and relative stabilities than are overlap repulsive terms (associated with the size mismatch effect). From the discussion of the distortions shown above, it is clear that this is even more the case when the substituted cation is triply charged. Size mismatch effects are important in explaining the different quantitative distortions induced by the three cations but do not influence the general distortion pattern appreciably. It is not surprising then that the NN configuration, which optimizes the electrostatic impurity−vacancies interactions, is the ground-state configuration irrespective of the impurity. It is also interesting that none of the impurities adopts an off-center equilibrium position, even though some calculations were carried out to test this possibility (the only difficulty with these calculations is that many of the lattice ions are not symmetry-equivalent anymore, which adds a lot of computational complexity. Apart from this, they are completely analogous to those shown in the previous subsections). This situation is different from the case of doubly charged substitutional impurities, which try to approach the electrostatic field of the only neighboring vacancy.[28] The presence of *two* vacancies, allocated symmetrically with respect to the impurity, prevents this approach from happening, which might well be the reason that the optical properties seem to be less affected by the vacancy effect in the case of triply charged impurities than in the case of doubly charged impurities.[34]

Another technical comment may be in order here. From Tables 1 and 2, we see that the fourth coordination shell of the impurity−vacancies complex experiences an appreciable distortion, so there exists the possibility that the distortions are not yet fully converged. To explicitly check this possibility, we included the ions at ($^3/_2$ 0 0) and equivalent positions, which are in the seventh coordination shell about the impurity in the $\mathbf{C}_1$ subset (this also increases the number of ions in the $\mathbf{C}_2$ subset, according to the convention explained in the Theory section). The displacement of these ions, although not completely negligible, was observed to be quite small (always smaller than 0.04 Å). Moreover, the energy difference between both defect configurations (0.49 eV) is very similar to the one previously quoted, so we conclude that the employed clusters provide at least a reasonable description of the lattice distortions about this kind of impurity.

IV. Summary

Our results indicate that the employment of a cluster approach, together with the aiPI model of electronic structure, is a useful way to disentangle the complicated distortion patterns occurring around aliovalent impurities in ionic crystals. This method has been applied to the specific case of KCl doped with As^{3+}, Sb^{3+}, and Bi^{3+}, providing the first ab initio quality results for this kind of system. Charge compensation has been achieved by introducing two cation vacancies into the host crystal, both in nearest-neighbor (NN) and next-nearest-neighbor (NNN) positions. The distortions have been shown to be mainly determined by electrostatic effects because the different sizes of the substitutional impurities is a less-important factor. Specifically, the size mismatch has no effect on the general distortion pattern, which is found to be the same in the three systems, and affects only the quantitative values of the distortions. Thus, even though the distortions are quite complicated, they can be explained mostly in terms of very simple (Coulombic) effects. None of the impurity cations adopts an off-center equilibrium position because of the symmetric allocation of the two cation vacancies. Our calculations also show that the NN defect configuration is energetically more stable than the NNN defect configuration irrespective of the size of the impurity, a result that may be helpful to the experimentalist in making a precise assignment of the absorption spectra.[35]

Acknowledgment. I thank the Ministry of Science and Technology of Spain for the concession of a postdoctoral grant.

References and Notes

(1) Blasse, G.; Grabmaier, B. C. *Luminescent Materials*; Springer Verlag: Berlin, 1995.
(2) Ranfagni, A.; Mugnai, D.; Bacci, M.; Viliani, G; Fontana, M. P. *Adv. Phys.* **1987**, *32*, 823.
(3) Jacobs, P. W. M. *J. Phys. Chem. Solids* **1991**, *52*, 35.
(4) Zazubovich, S. *Int. J. Mod. Phys. B* **1994**, *8*, 985.
(5) Barkyoumb, J. H.; Mansour, A. N. *Phys. Rev. B* **1992**, *46*, 8768.
(6) Pong, W. F.; Mayanovic, R. A.; Bunker, B. A.; Furdyna, J. K.; Debska, U. *Phys. Rev. B* **1990**, *41*, 8440.
(7) Zaldo, C.; Prieto, C.; Dexpert, H.; Fessler, P. *J. Phys.: Condens. Matter* **1991**, *3*, 4135.
(8) Aramburu, J. A.; Moreno, M.; Cabria, I.; Barriuso, M. T.; Sousa, C.; de Graaf, C.; Illás, F. *Phys. Rev. B* **2000**, *62*, 13356. Sousa, C.; de Graaf, C.; Illás, F.; Barriuso, M. T.; Aramburu, J. A.; Moreno, M. *Phys. Rev. B* **2000**, *62*, 13366.
(9) Aguado, A.; Ayuela, A.; López, J. M.; Alonso, J. A. *Phys. Rev. B* **1998**, *58*, 11964.
(10) Aguado, A.; López, J. M.; Alonso, J. A. *Phys. Rev. B* **2000**, *62*, 3086.
(11) Aguado, A. *J. Chem. Phys.* **2000**, *113*, 8680.
(12) Tsuboi, T.; Jacobs, P. W. M. *J. Phys. Chem. Solids* **1991**, *52*, 69.
(13) Aguado, A. *J. Phys.: Condens. Matter* **2001**, *13*, 8015.
(14) Tsuboi, T.; Nakai, Y.; Oyama, K.; Jacobs, P. W. M. *Phys. Rev. B* **1973**, *8*, 1698.
(15) Oyama, K.; Jacobs, P. W. M. *J. Phys. Chem. Solids* **1975**, *36*, 1375. Oyama, K.; Jacobs, P. W. M. *J. Phys. Chem. Solids* **1975**, *36*, 1383.
(16) Corish, J.; Quigley, J. M.; Jacobs, P. W. M.; Catlow, C. R. A. *Philos. Mag. A* **1981**, *44*, 13.
(17) Kamashina, Y.; Sivasankar, V. S.; Jacobs, P. W. M. *J. Chem. Phys.* **1982**, *76*, 4677.
(18) Sivasankar, V. S.; Kamashina, Y.; Jacobs, P. W. M. *J. Chem. Phys.* **1982**, *76*, 4681.
(19) Corish, J.; Catlow, C. R. A.; Jacobs, P. W. M.; Ong, S. H. *Phys. Rev. B* **1982**, *25*, 6425.
(20) Catlow, C. R. A.; Chadwick, A. V.; Corish, J. *J. Solid State Chem.* **1983**, *48*, 65.
(21) Schmitt, K.; Jacobs, P. W. M.; Stillman, M. J. *J. Phys. C: Solid State Phys.* **1983**, *16*, 603.
(22) Dang, L. S.; Jacobs, P. W. M.; Simkin, D. J. *J. Phys. C: Solid State Phys.* **1985**, *18*, 3567.
(23) Baranov, P. G.; Vetrov, V. A.; Romanov, N. G.; Topa, V. *Phys. Status Solidi B* **1986**, *136*, 699.
(24) Tsuboi, T.; Kamewari, T. *J. Phys.: Condens. Matter* **1994**, *6*, 8613.
(25) Nagirnyi, V.; Stolovich, A.; Zazubovich, S.; Jaanson, N. *Phys. Rev. B* **1994**, *50*, 3553.
(26) Macalik, B.; Siu-Li, M.; Zazubovich, S. *Radiat. Eff. Defects Solids* **1998**, *147*, 11.
(27) Tsuboi, T. *Electrochem. Solid-State Lett.* **2000**, *3*, 200.
(28) Aguado, A. *J. Chem. Phys.* **2001**, *114*, 5256. *Phys. Status Solidi B* **2002**, *229*, 1335.
(29) Radharkrishna, S.; Karguppikar, A. M. *J. Phys. Chem. Solids* **1973**, *34*, 1497.
(30) Choi, K. O.; Lee, S. W.; Bea, H. K.; Jung, S. H.; Chang, C. K.; Kang, J. G. *J. Chem. Phys.* **1991**, *94*, 6420.
(31) Höner, J.; Siederdissen, Z.; Fischer, F. *Phys. Status Solidi B* **1971**, *48*, 215.
(32) Hughes, A. E.; Pells, G. P. *Phys. Status Solidi B* **1975**, *71*, 707.
(33) Radharkrishna, S.; Srinivasa Setty, R. S. *Phys. Rev. B* **1976**, *14*, 969.
(34) Tsuboi, T.; Ahmet, P.; Kang, J. G. *J. Phys.: Condens. Matter* **1992**, *4*, 531.

(35) Kang, J. G.; Yoon, H. M.; Chun, G. M.; Kim, Y. D.; Tsuboi, T. *J. Phys.: Condens. Matter* **1994**, *6*, 2101.
(36) Luaña, V.; Pueyo, L. *Phys. Rev. B* **1990**, *41*, 3800.
(37) Luaña, V.; Recio, J. M.; Pueyo, L. *Phys. Rev. B* **1990**, *42*, 1791.
(38) Pueyo, L.; Luaña, V.; Flórez, M.; Francisco, E. In *Structure, Interactions and Reactivity*; Fraga, S., Ed.; Elsevier: Amsterdam, 1992; Vol. B, p 504.
(39) Luaña, V.; Flórez, M.; Francisco, E.; Martín Pendás, A.; Recio, J. M.; Bermejo, M.; Pueyo, L. In *Cluster Models for Surface and Bulk Phenomena*; Pacchioni, G., Bagus, P. S, Parmigiani, F., Eds.; Plenum Publishing: New York, 1992; p 605.
(40) Luaña, V.; Martín Pendás, A.; Recio, J. M.; Francisco, E. *Comput. Phys. Commun.* **1993**, *77*, 107.
(41) Blanco, M. A.; Martín Pendás, A.; Luaña, V. *Comput. Phys. Commun.* **1997**, *103*, 287.
(42) Huzinaga, S.; Cantu, A. A. *J. Chem. Phys.* **1971**, *55*, 5543.
(43) Huzinaga, S.; McWilliams, D.; Cantu, A. A. *Adv. Quantum Chem.* **1973**, *7*, 183.
(44) Luaña, V.; Flórez, M. *J. Chem. Phys.* **1992**, *97*, 6544.
(45) Luaña, V.; Flórez, M.; Pueyo, L. *J. Chem. Phys.* **1993**, *99*, 7970.
(46) Flórez, M.; Blanco, M. A.; Luaña, V.; Pueyo, L. *Phys. Rev. B* **1994**, *49*, 69.
(47) Clementi, E.; Roetti, C. *At. Data Nucl. Data Tables* **1974**, *14*, 177.
(48) McLean, A. D.; McLean, R. S. *At. Data Nucl. Data Tables* **1981**, *26*, 197.
(49) Jiang, H.; Costales, A.; Blanco, M. A.; Gu, M.; Pandey, R.; Gale, J. D. *Phys. Rev. B* **2000**, *62*, 803.
(50) Madden, P. A.; Wilson, M. *Chem. Soc. Rev.* **1996**, *25*, 399.
(51) Jemmer, P.; Wilson, M.; Madden, P. A.; Fowler, P. W. *J. Chem. Phys.* **1999**, *111*, 2038.
(52) Hutchinson, F.; Wilson, M.; Madden, P. A. *J. Phys.: Condens. Matter* **2000**, *12*, 10389.
(53) Domene, C.; Fowler, P. W.; Wilson, M.; Madden, P. A.; Wheatley, R. J. *Chem. Phys. Lett.* **2001**, *333*, 403.
(54) Aguado, A.; López-Gejo, F.; López, J. M. *J. Chem. Phys.* **1999**, *110*, 4788. Aguado, A.; López, J. M. *J. Phys. Chem. B* **2000**, *104*, 8398.